Raman spectra and lattice dynamics of single-crystal $\alpha - Bi_2O_3$

1997 J. Phys.: Condens. Matter 9 4967

(http://iopscience.iop.org/0953-8984/9/23/020)

J. Phys.: Condens. Matter **9** (1997) 4967–4978. Printed in the UK PII: S0953-8984(97)76836-X

Raman spectra and lattice dynamics of single-crystal α-Bi_2O_3

V N Denisov†, A N Ivlev†, A S Lipin†, B N Mavrin† and V G Orlov‡

† Institute for Spectroscopy, Russian Academy of Science, 142092 Troitsk, Moscow Region, Russia

‡ Kurchatov Institute Russian Research Centre, 123182 Moscow, Russia

Received 1 August 1996, in final form 5 March 1997

Abstract. Polarized Raman spectra of oriented monoclinic single crystals of α-Bi_2O_3 have been obtained at temperatures of 20–650 K in the region 15–3500 cm^{-1}. The assignment of the Raman bands to the A_g and B_g modes was given. The photoinduced reduction of the Raman intensity was observed after heating a crystal above 500 K, and cooling it down to room temperature, under laser irradiation. A lattice dynamical analysis based on two-particle interatomic potentials and a rigid-ion model was performed. These potentials were consistent with the Raman and IR data, besides which they showed a stable dynamics throughout the Brillouin zone, and yielded the minimum of internal forces and pressures in the crystal lattice. The phonon dispersion curves, and the projected and total densities of phonon states were calculated.

1. Introduction

Recently the sesquilateral oxide Bi_2O_3 has attracted attention, not only because of its polymorphic structure [1], but also as one of the initial components used in the synthesis of high-temperature superconductors (HTSC). Moreover, unusual magnetic and electrical properties, such as the existence of internal magnetic fields [2], a positive value of the magnetization in a weak magnetic field at low temperatures, the high sensitivity of the magnetization to the thermomagnetic history [3], and the presence of a linear magnetoelectric effect [3], were found for α-Bi_2O_3. Anomalous physical properties, such as exothermal maxima of the DTA and DSC curves, and a sharp increase of the real part of the dielectric function, were observed for α-Bi_2O_3 at temperatures of 450–570 K [4]. Since the structural phase transition was not detected in this temperature range, it was suggested [4] that these anomalies were related to changes of the electronic structure of α-Bi_2O_3 at temperatures of 450–570 K.

Many physical properties of crystals are determined by the interatomic interactions and lattice dynamics. Complete information on the lattice dynamics can be obtained from the study of vibrational spectra throughout the Brillouin zone (BZ), which is possible only by means of inelastic neutron scattering. However, this method is effective only for simple crystals with a small number of phonon branches. The application of this method to the phonon dispersion study of the α-Bi_2O_3 crystal seems difficult, since one should expect 60 phonon branches in the small spectral range of 50–550 cm^{-1}. In this situation the methods of Raman scattering and IR spectroscopy enable one to obtain information on vibrational

0953-8984/97/234967+12$19.50

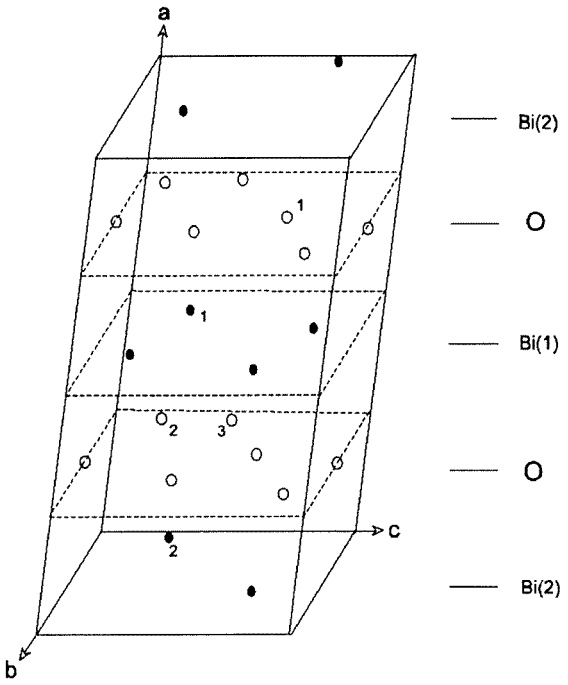

Figure 1. The unit cell of the α-Bi_2O_3 crystal; layers of Bi(1) atoms at $x \approx 0.5$, and Bi(2) atoms at $x \approx 0$ and $x \approx 1$, as well as oxygen atoms at $x \approx 0.25$ and $x \approx 0.75$ are shown. The inequivalent bismuth and oxygen atoms [1] are labelled with numbers.

spectra in the BZ centre, which becomes the main source of data for lattice dynamics simulation.

Four polymorphs of Bi_2O_3 are known. The low-temperature one is a monoclinic α-phase: space group C_{2h}^5 ($P2_1/c$); $Z = 4$; all of the atoms are in a general position (figure 1) [1]. It transforms to the cubic δ-phase at 729 °C. The other phases (β and γ) are metastable, and may be obtained by cooling (to 650 °C for the γ-phase, and to 639 °C for the β-phase). Both phases transform to the α-phase in the region 650–500 °C [1].

According to the group theory analysis, the vibrational representation of the optical vibrations in the crystal α-Bi_2O_3 may be represented as [5]

$$\Gamma = 15A_g + 15B_g + 14A_u + 13B_u. \tag{1}$$

Thus, one should expect $15A_g$ and $15B_g$ modes in the Raman spectra of α-Bi_2O_3

So far the Raman spectra of α-Bi_2O_3 have been investigated only for powder samples [5–8], and not all of the modes have been detected. Only in [8] was an attempt made to assign the observed bands to some vibrational types, using the normal-mode analysis made by the GF technique for the BZ centre. Since the α-Bi_2O_3 crystal has very low symmetry, one should expect 11 Bi–O bonds with lengths below 3 Å, 12 O–O bonds (<3.3 Å), and 13 Bi–Bi bonds (<4.5 Å), with different lengths as regards nearest neighbours only. The GF technique leads to one both handling many parameters, and using unsubstantiated dependences of force constants on bond lengths, as was done in [8].

In this paper, for the first time, polarized Raman spectra of oriented single crystals of α-Bi_2O_3 are obtained. Using these spectra and IR spectra of α-Bi_2O_3 single crystal [9], we have performed a lattice dynamical analysis based on the rigid-ion model and two-

particle potentials. We used an extended set of starting spectroscopic data, as compared with that used in [8], carried out a lattice dynamical analysis throughout the BZ, and found the force field that not only accorded with the Raman and IR data, but also yielded positive frequencies through the BZ, minimized forces and stresses in the crystal lattice, and satisfactorily described the measured density of phonon states.

In this paper, in section 2 we describe the experiment and the Raman spectra obtained, in section 3 we outline the interatomic potential, and in section 4 we discuss the results.

2. The experiment and the Raman spectra

The single crystals of α-Bi_2O_3 were obtained by hydrothermal synthesis in alkaline water solutions. Bi_2O_4 was used as the charge. The synthesis was carried out in an autoclave, at a temperature of 573 K, and under a pressure of 80 MPa. The unit-cell parameters of the monoclinic crystal lattice were in agreement with published data [1]. According to the results of the electron probe microanalysis performed with the CAMEBAX-301 spectrometer, the contamination of the crystal did not exceed 0.01 wt%.

The crystal of α-Bi_2O_3 investigated had a well-determined natural ac-face (a, b, and c are the crystallographic axes, and $\boldsymbol{b}||C_2$). We could choose the scattering geometries to separate the A_g and B_g modes in the Raman spectra. The Raman spectra were obtained in the backscattering geometries: $a(bb)\bar{a}$ and $a(c'c')\bar{a}$ for the observation of the A_g modes, as well as $a(bc')\bar{a}$ and $a(c'b)\bar{a}$ for the study of the B_g modes, where c' is a direction in the ac-plane perpendicular to the a-axis. Because of the strong double refraction in the biaxial crystal α-Bi_2O_3, the Raman spectra were very sensitive to the orientation of the crystal with respect to the crystallographic axes.

Figure 2 represents the polarized Raman spectra of single-crystal α-Bi_2O_3, at room temperature. The Raman bands with frequencies above 200 cm^{-1} are very broad. Also, we could not avoid a depolarization of the Raman bands due to the double refraction and misorientation of the crystal. For example, the strong lines in the $a(bb)\bar{a}$ scattering geometry appear as weak bands in the $a(bc')\bar{a}$ geometry (figure 2). Therefore, the correct assignment of bands to the A_g or B_g modes requires careful analysis of the Raman spectra in all four scattering geometries.

Additional information was obtained from the Raman spectrum for α-Bi_2O_3 at low temperatures. We could not obtain polarized Raman spectra of good quality, because it was difficult to orient a small biaxial crystal accurately in the cryostat. The spectrum of the α-Bi_2O_3 powder at 20 K (figure 3) exhibited some bands that were not seen at room temperature, due to broadening and overlapping. For example, the band at 91 cm^{-1} appearing as a single band at room temperature revealed two components at 95 and 97 cm^{-1}. Furthermore, we found 137 (at 300 K) $\rightarrow$ 137 + 139 (at 20 K), 4150 $\rightarrow$ 150 + 151, 210 $\rightarrow$ 210 + 212, 280 $\rightarrow$ 280 + 282, 314 $\rightarrow$ 317 + 340, 447 $\rightarrow$ 413 + 435 + 459 + 468, and 529 $\rightarrow$ 525 + 529 cm^{-1}. Therefore, we suggest an absence of structural transitions with decreasing temperature up to 20 K. For Raman excitation with the 6328 Å laser line, we could confidently record the Raman spectra in the region from 15 cm^{-1}, but we have not found bands below 50 cm^{-1}.

The results of our assignment of the observed Raman frequencies to the A_g or B_g modes are represented in table 1. This assignment is based on the polarized spectra at room temperature, and the temperature behaviour of the spectra of α-Bi_2O_3 crystal and powder. Table 1 represents the frequencies at room temperature.

We carried out a number of experiments to investigate the temperature dependence of the Raman spectra of α-Bi_2O_3 samples above room temperature. Heating from room

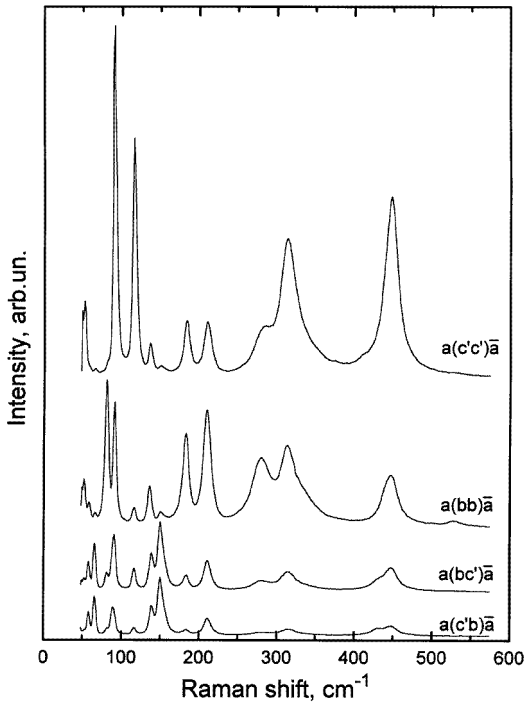

Figure 2. Polarized Raman spectra of single-crystal α-Bi_2O_3 in various backscattering geometries, at room temperature.

temperature up to 650 K was performed at rates of 10–100 K min^{-1}, and the same rates were used for cooling. In these experiments we used α-Bi_2O_3 powder, since single crystals suffered a structure failure at $T > 500$ K. Three excitation wavelengths, 6328, 5145, and 4880 Å, with different incident power densities, were used to carry out the Raman measurements. The evolution of the spectra was not affected by the heating and cooling rates. It was found that the behaviour of the spectra with 6328 Å excitation differed significantly from that with 5145 and 4880 Å excitation.

Using 6328 Å excitation during heating, we have not observed other changes in the Raman spectra, except the temperature broadening and a small shift of the bands. After cooling to room temperature, the Raman intensity returned to the original state within the experimental accuracy. Neither the presence nor the absence of laser irradiation during heating or cooling changed this result.

With 5145 and 4880 Å excitation, we have studied two heating–cooling cycles: with cooling under laser irradiation (**I**), and with cooling without laser irradiation (**D**). The Raman spectra after heating up to 650 K did not depend on the presence or absence of laser irradiation or on the heating–cooling cycles, but the Raman intensity significantly dropped while heating the sample (figure 3). The absorption edge of the α-Bi_2O_3 crystal is near 4500 Å at room temperature, according to our measurements of the optical transmission. Therefore one can suggest that the drop of the Raman intensity is due to an increased electronic absorption after heating.

The intensity of the spectra after cooling to room temperature was affected by the presence of laser irradiation. The Raman intensity after cooling in an **I**-type cycle was found to be several times less than that after cooling in a **D**-type cycle with an incident

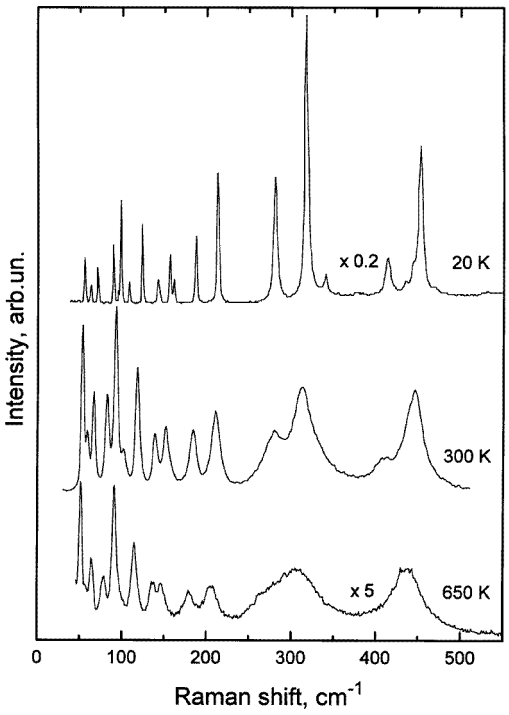

Figure 3. Raman spectra of the α-Bi_2O_3 powder, at various temperatures.

power density of $\sim$1 kW cm^{-2}. This drop of intensity decreased with the diminution of the laser power density. Therefore, one can consider that these intensity changes occur due to photo-induced processes related to excitations in the electronic subsystem of α-Bi_2O_3.

3. The interatomic potential in the rigid-ion model

As we already mentioned, the fact that there are a lot of atoms in the unit cell, and the low symmetry of the α-Bi_2O_3 crystal, result in one handling a great number of force constants. Since the experimental information concerning phonons in α-Bi_2O_3 is insufficient, we tended to reduce the number of parameters describing the force field. In this situation it was expedient to carry out lattice dynamical analysis based on interatomic potentials within the framework of the rigid-ion model.

In our rigid-ion model, each atom k had the charge q_k and the parameters of the interatomic interaction with neighbouring atoms. The model considered both long-range (Coulomb) and short-range forces. The Coulomb coefficients were calculated by means of the Ewald method. The short-range forces were represented by a central potential that was a sum of Born–Mayer and van der Waals potentials:

$$\Phi_{kk'}(r_{ij}) = b_{kk'} \exp(-r_{ij}/\rho_{kk'}) - C_{kk'}/r_{ij}^6 \tag{2}$$

where r_{ij} is the distance between atoms i and j of types k and k' respectively; $b_{kk'}$, $\rho_{kk'}$, and $C_{kk'}$ are parameters of the potential.

The unit cell of α-Bi_2O_3 contains five inequivalent atoms: two bismuth atoms, Bi(1) and Bi(2), and three oxygen atoms, O(1), O(2), and O(3) (see figure 1). For the sake of

Table 1. Measured and calculated phonon frequencies (cm^{-1}) at $\boldsymbol{k} = 0$ in α-Bi_2O_3.

Experiment				Calculation					
						TO		LO	
A_g[a]	B_g[a]	A_u[b]	B_u[b]	A_g	B_g	A_u	B_u	A_u	B_u
52	58	—	—	40	57	0	0	0	0
58	66	37[c]	—	62	62	32	0	33	0
81	89	58	58[c]	81	88	52	57	54	58
91	91	—	—	91	92	82	66	85	72
117	116	99	—	103	109	97	90	97	97
137	139	—	102[c]	126	131	119	123	120	146
151	150	130	145	153	143	130	145	136	208
183	184	153	175	188	232	145	149	185	221
210	212	185	179	228	244	207	215	210	246
280	282	209	222	290	278	223	254	268	313
314	314	280	280	354	372	295	334	346	359
413	432	314	362	369	418	359	339	368	374
447	447	—	401[c]	464	469	391	367	397	402
468[d]	468[d]	486	414[c]	482	479	430	433	436	434
529	525[d]	544[c]	504[c]	536	532	510	504	511	506

[a] Our data.
[b] From reference [9].
[c] Infrared TO modes are included in the fitting.
[d] Raman modes are excluded from the fitting.

simplicity, we supposed that the crystal has only two types of atom, i.e. the atoms Bi(1) and Bi(2), and the atoms O(1), O(2), and O(3) were regarded as identical. So, only one charge q(Bi) was unknown, because the charge q(O) was determined by the neutrality condition. As in [10], we considered the van der Waals interaction between oxygen atoms only. Hence, within the framework of our model, the interatomic potential was defined by eight parameters: b(Bi–Bi), b(Bi–O), b(O–O), ρ(Bi–Bi), ρ(Bi–O), ρ(O–O), C(O–O), and q(Bi), where b, ρ, and C are parameters of the interatomic potential (2) for the pairs of atoms indicated in brackets.

Earlier, the authors of [8, 11] assumed a predominantly covalent character of Bi–O bonds in this crystal. It has been shown [10] that in this case the lattice dynamics is more stable when one adds a covalent potential to (2):

$$\Phi^{cov}(r_{ij}) = -a_1 \exp(-a_2(r_{ij} - r_0)^2) \tag{3}$$

which represents an additional interaction between the Bi and O atoms with covalent bonding. The potential (3) requires three supplementary parameters: a_1, a_2, and r_0. In section 4 we will discuss this potential in a lattice dynamical analysis of α-Bi_2O_3.

In order to agree the chosen parameters not only with the measured phonon frequencies, but also with the crystalline structure, we tried to satisfy the static equilibrium conditions [12] that are equivalent to the absence of forces and stresses in the crystal:

$$\sum_i \Phi'(r_{ij}) r_{ij,\alpha}/r_{ij} + F_\alpha(j) = 0 \tag{4}$$

$$\frac{1}{2}\sum_{ij} \Phi'(r_{ij}) r_{ij,\alpha} r_{ij,\beta}/r_{ij} + f_{\alpha\beta} = 0 \tag{5}$$

where Φ' is the first derivative of the short-range potentials; α and β are the Cartesian

coordinates; F and f are the Coulomb contributions. In fact, the requirement of the rigorous application of equations (4) and (5) prevented us from obtaining the frequencies close to the measured values. This is due to both deficiencies of our model and errors in the measured structural parameters [1] that we used in the calculations. Therefore, we fitted the computed frequencies to the experimental ones, preserving forces and stresses, at reasonably small values.

4. Discussion of the results

In the calculations, we took into consideration interactions between nearest neighbours only. According to structural data [1], the minimal interatomic Bi–Bi distances fall in the range 3.4–4.4 Å, and the next Bi–Bi distances are over 5 Å. Therefore, the cut-off radius for the Bi–Bi interactions was chosen as 4.5 Å. In the same way, cut-off radii of 3.0 and 3.3 Å for the Bi–O and O–O interactions, respectively, were determined.

We have used only the Raman and IR data to define the potential parameters. Besides this, we have compared the computed and measured densities of phonon states. 27 Raman and 7 IR frequencies were employed in the fitting (see table 1).

Within the framework of our model, we have performed a lattice dynamical analysis for several situations:

(1) the absence of charges on atoms, i.e. $q_k = 0$;
(2) the presence of charges on atoms; and
(3) the addition of the covalent potential (3) for the Bi–O interaction.

The assumption that $q_k = 0$ was used earlier in the normal-mode analysis with the GF technique [8]. We could obtain both the stable dynamics (real phonons throughout the BZ), and a good fitting at the Γ point within our model at $q_k = 0$, taking into account the equations (4) and (5). In this case, a large $C_{kk'}$-parameter (5800 eV), and hence large values of $b_{kk'}$, were needed for the fitting. But the magnitudes of the longitudinal ($L_{kk'}$) and transverse ($T_{kk'}$) force constants defined in terms of the derivatives of the potential (2) as

$$L_{kk'} = \Phi''_{kk'}(r_{ij}) \qquad T_{kk'} = \Phi'_{kk'}(r_{ij})/r_{ij} \tag{6}$$

had reasonable values for the nearest interionic interactions. The set of force constants that were averaged over the group of nearest neighbours, and gave a qualitatively correct description of the vibrational spectrum, are represented in table 2. The force constants from reference [8] are also given for comparison. It is seen that all of the two-particle force constants are substantially larger in [8].

However, the assumption that $q_k = 0$ did not accord with the measured anisotropy of the dielectric function in the basal ac-plane, which was perpendicular to the b-axis. From IR data [9], the dielectric function along the a-axis was 1.5 less than it was for the direction perpendicular to the a-axis in the ac-plane.

The anisotropy of the dielectric function could be obtained on the assumption that $q_k \neq 0$. In this case our model had eight parameters (see section 3). The starting model parameters for the O–O and Bi–O interactions were taken from the lattice dynamical analysis of bismuth HTSC: 0.3 Å for $\rho_{kk'}$ and 3000 eV for $b_{kk'}$. Equations (4) and (5) were also included in the fitting. The following main results were obtained.

(1) The stable dynamics required the consideration of all of the different interactions, Bi–Bi, Bi–O, and O–O.

Table 2. The force constants of the two-particle interactions obtained from the GF matrix method [8] and our rigid-ion model ($q(k) = 0$). FC: force constants obtained using the GF technique [8]; L and T: longitudinal and transverse force constants (equation (6)); d, the region of averaged bonds.

	FC (N m^{-1})	d (Å)	L (N m^{-1})	T (N m^{-1})	d (Å)
Bi–Bi	45.9	3.46	24.1	−1.6	3.46–3.73
	43.7	3.56	3.1	−0.2	3.91–4.38
Bi–O	111.5	2.10–2.29	97.1	−6.9	2.13
	63.2	2.48–2.80	52.5	−3.6	2.20–2.28
			6.3	−0.4	2.42–2.79
O–O	54.7	2.79–2.87	38.1	−0.5	2.76–2.89
	32.8	3.07–3.09	30.6	3.9	3.08–3.24
	27.9	3.23			

(2) The $C_{kk'}$-parameter of the van der Waals potential was essentially smaller for $q_k \neq 0$, and a minimum of forces and stresses was reached at $C_{kk'} = 1300$ eV.

(3) We could not find parameters $b_{kk'}$, $\rho_{kk'}$, and $C_{kk'}$ that would yield a stable dynamics for $q(\mathrm{Bi}) > +1.5$. The good fitting was at $q(\mathrm{Bi}) = +1.26$ and $q(\mathrm{O}) = -0.84$. The small charges on the atoms indicate that the ionicity of the Bi–O bonds is not large.

Since the Bi–O bond is covalent, the addition of covalent potential (3) to potential (2) seemingly should improve the fitting. However, the addition of potential (3) did not improve the fitting, but the agreement between the calculated and measured dielectric functions, and the density of phonon states was worsened. Therefore, we will discuss the results of calculations without the covalent potential for $q_k \neq 0$.

Table 3. Parameters of the rigid-ion model. $q(k)$: ionic charge; $b_{kk'}$, $\rho_{kk'}$: parameters of the Born–Mayer potential; $C_{kk'}$: the parameter of the van der Waals potential.

	$q(k)$	$b_{kk'}$ (eV)	$\rho_{kk'}$ (Å)	$C_{kk'}$ (eV Å^6)
Bi	1.26			
O	−0.84			
Bi–Bi		6600	0.34	
Bi–O		5200	0.22	
O–O		6900	0.35	1300

The parameters of the potential are given in table 3. The internal forces acting on the Bi and O atoms fall in the range 0.05–0.32 eV Å^{-1}, and the internal pressures did not exceed 5 GPa, which was a reasonable limit [13]. These values could be diminished at the expense of a substantial disagreement of the computed and measured frequencies.

First, let us consider the results of the calculation for the BZ centre. The vibrational spectrum of α-Bi_2O_3 contains g and u modes (equation (1)). The dipole u modes split into transverse (TO) and longitudinal (LO) components, and their frequencies depend on the direction of the $\boldsymbol{k}$-wavevector of the modes. It is easy to find the TO and LO frequencies of the A_u modes polarized along the b-axis. Taking $\boldsymbol{k}||\boldsymbol{b}$ we get the LO(A_u) modes, and we get the TO(A_u) modes with $\boldsymbol{k}\perp\boldsymbol{b}$.

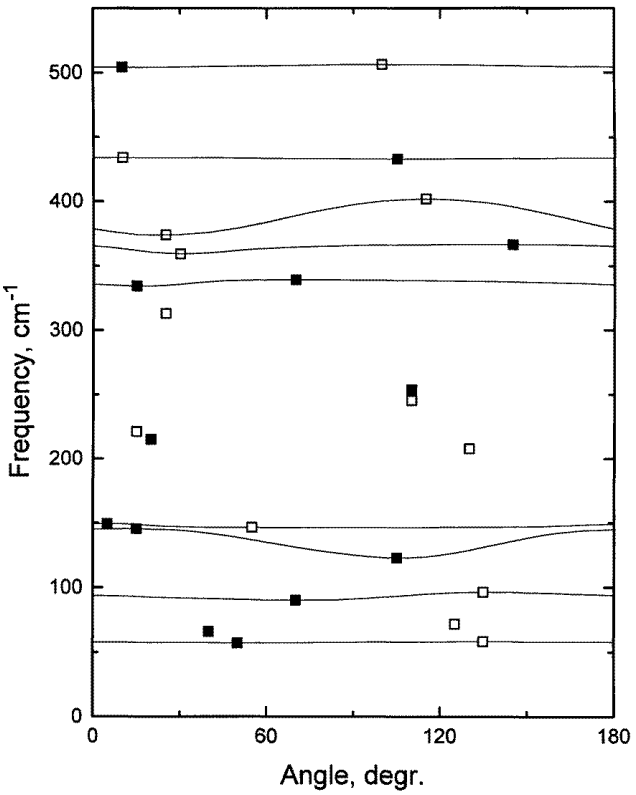

Figure 4. The dependences of the frequencies of the B_u modes on the angle between the *c*-axis and the direction of the phonon wavevector located in the *ac*-plane; ■ and □ show positions of TO and LO frequencies respectively. The TO frequencies are found from calculations for $\boldsymbol{k}||\boldsymbol{b}$ (see the text), and they coincide with some extrema on branches in this figure. The LO frequencies are defined as other extrema on these branches.

The TO frequencies of the B_u modes polarized in the *ac*-plane are calculated for $\boldsymbol{k}||\boldsymbol{b}$. The polarization of the B_u modes is linear, and each mode has its own direction. In order to find the LO(B_u) modes, we have calculated the frequency dependences of the B_u modes on the ϑ-direction of $\boldsymbol{k}$ in the *ac*-plane, measuring the ϑ-angle from the *c*-axis (see figure 4). In this case, the frequencies of the B_u modes, like those of the mixed phonons in uniaxial crystals, vary within the limits for TO–LO, TO–TO, or TO–LO frequencies, depending on the relationship between the electrostatic and anisotropic forces. Since the frequencies of the TO(B_u) modes are known, the LO(B_u) frequencies can be determined from these dependences.

The calculated TO and LO frequencies of the A_u and B_u modes, and the A_g and B_g frequencies, are given in table 1, and compared with the experimental frequencies. In this table the calculated LO frequencies of the A_g and B_g modes are arranged in the order of increasing frequencies. We have obtained good agreement between the calculated and measured frequencies for g modes, but not such good agreement for TO modes. Such a disagreement for the TO modes may be due to difficulties encountered in the IR measurements in biaxial crystals. Besides this, the agreement could be improved by increasing the number of variable parameters, considering that the Bi(1) and Bi(2) atoms,

as well as the O(1), O(2), and O(3) atoms, are actually different.

The calculated TO and LO frequencies of the u modes enabled us to estimate the oscillator strengths S_i, and the vibrational contribution to the static dielectric function ε_0 [14]:

$$S_i = (\varepsilon_\infty/\omega_{TO,i}^2)(\omega_{LO,i}^2 - \omega_{TO,i}^2)\prod_{j\neq i}\frac{\omega_{LO,j}^2 - \omega_{TO,i}^2}{\omega_{TO,j}^2 - \omega_{TO,i}^2} \tag{7}$$

$$\varepsilon_0 = \varepsilon_\infty + \sum_i S_i. \tag{8}$$

The equations (7) and (8) allow us to find $\varepsilon_0^{\parallel}$ along the *b*-axis from the data for the A_u modes: $\varepsilon_0^{\parallel} = 4.86\varepsilon_\infty^{\parallel}$. The determination of $\varepsilon_0^{\perp}$ from the data for the B_u modes is not so simple, because the directions of the phonon polarization for each mode should be considered. Nevertheless, one can estimate that $\varepsilon_0^{\perp}$ is greater than $\varepsilon_0^{\parallel}$, which is consistent with experiment [9].

As was noted earlier [8], the motion of atoms in each mode is very complex to describe. We found that there is a boundary near 120 cm^{-1}. Below 120 cm^{-1} the modes are due to displacements of the Bi atoms only, while above 150 cm^{-1} they are mainly due to displacements of the oxygen atoms. This will be demonstrated below on the basis of the spectral distribution of the density of phonon states. As is seen from figures 2 and 3, the oxygen modes show broad bands in comparison with the bismuth modes, which provides evidence for the strong anharmonicity of the oxygen modes.

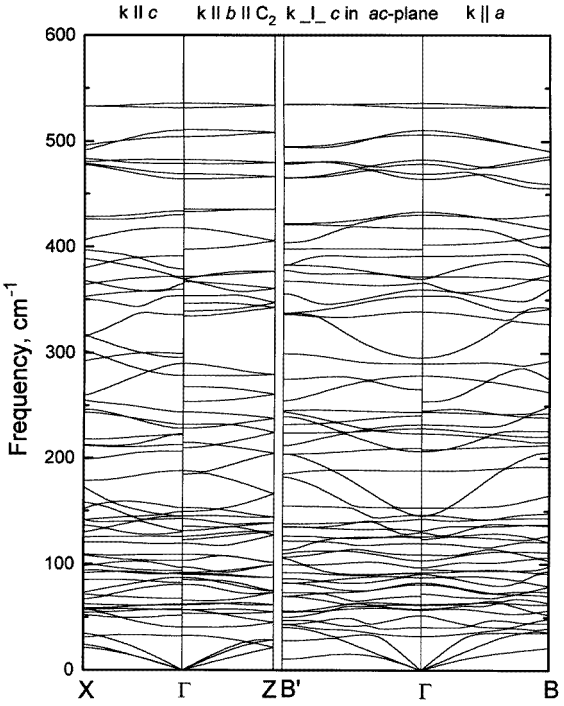

Figure 5. Phonon dispersion curves of α-Bi_2O_3 for various directions in the Brillouin zone.

Figure 5 shows the calculated dispersion curves in four directions of the BZ, along the crystallographic *a*-, *b*-, and *c*-axes, and perpendicularly to the *c*-axis in the *ac*-plane.

One can see that the dispersion branches are stable along these directions. This is far from trivial, since the α-Bi_2O_3 structure tends to cause acoustic phonon instabilities. There are only very narrow windows in the parameter space of the potentials used, which leads to stable dispersion curves throughout the BZ. First of all, an instability appears in the acoustical branch along Γ–B on the BZ edge. Let us note two features of the dispersion curves. Firstly, at the Z point on the BZ edge, the irreducible representations should be doubly degenerate for the C_{2h}^5 group [15], as is clearly seen in figure 5. Secondly, at the Γ point, for the X–Γ–Z direction (figure 5), some dispersion curves exhibit jumps due to the fact that there are LO(A_u) and TO(B_u) modes at the Γ point for the Γ–Z direction, while there are TO(A_u) and mixed B_u modes at this point for the Γ–X direction. At the Γ point for the B–Γ–B′ direction, only the B_u modes show jumps due to a change of the ϑ-angle, for the $\boldsymbol{k}$-wavevector in the ac-plane.

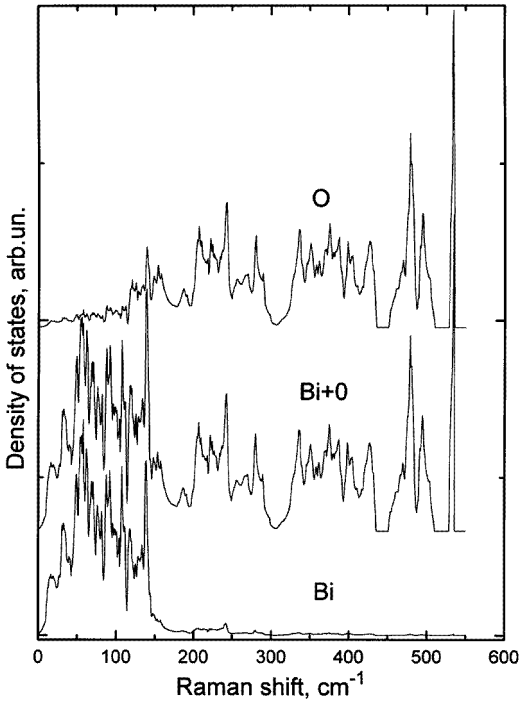

Figure 6. The density of phonon states in α-Bi_2O_3; the traces labelled O and Bi are the projected densities for modes with displacements of O and Bi atoms, respectively; the trace labelled Bi+O is the total density of phonon states in α-Bi_2O_3.

Using our model, we have calculated also the projected and total densities of phonon states (see figure 6). The experimental total density of states found from the measurements of inelastic neutron scattering [16] contains intense peaks at 59, 218, 344, 424, and 532 cm^{-1}, and weak shoulders at 102, 123, 165, and 195 cm^{-1}. These maxima correlate with the calculated ones, but the additional peaks near 280 and 480 cm^{-1} that are not seen in the measured density are present in the calculated function of the density of phonon states. The projected densities of states (figure 6) show the contributions of the Bi and O atoms, and provide information concerning the displacements of these atoms in vibrations depending on the mode frequencies. There are three regions in the phonon density of states (figure 6). The

Bi atoms participate mainly in vibrations below 120 cm^{-1}, while modes above 150 cm^{-1} are due to displacements of the O atoms. Modes in the range 120–150 cm^{-1} are defined by the displacements of both Bi and O atoms.

5. Conclusions

For the first time, polarized Raman spectra of single-crystal α-Bi_2O_3 are studied, and the assignment of the bands to certain vibrational modes is carried out. It is found that the frequencies of A_g and B_g modes are grouped in pairs. The Raman spectra of α-Bi_2O_3 at helium temperature are obtained also. It is shown that, in the temperature range investigated, no unexpected changes in the spectra occur, except the notable band narrowing and more distinct exhibiting of overlapping bands. A lattice dynamical simulation is performed within the approximation of interatomic potentials and the rigid-ion model, utilizing Raman and IR experimental data. It is revealed that a stable lattice dynamics can be obtained by considering interactions only between nearest atoms (Bi–Bi, Bi–O, and O–O). The phonon dispersion curves, and the TO and LO frequencies of the dipole modes are computed. The dielectric function in the basal plane is shown to be anisotropic, according with experimental results. The projected and total densities of phonon states are calculated.

References

[1] Harwig H A 1978 *Z. Anorg. Allg. Chem.* **444** 151
[2] Kravchenko E A and Orlov V G 1994 *Z. Naturf.* a **49** 418
[3] Kharkovskii A I, Nizhankovskii V I, Kravchenko E A and Orlov V G 1997 *Z. Naturf.* a **51** at press
[4] Orlov V G, Bush A A, Ivanov S A and Zhurov V V 1997 *Int. Conf. on the Physics and Chemistry of Molecular and Oxide Superconductors (Karlsruhe, 1996)* submitted
[5] Betsch R J and White W B 1978 *Spectrochim. Acta* A **34** 505
[6] Popovic Z V, Thomsen C, Cardona M, Liu R, Stanisic G, Kremer R and Konig W 1988 *Solid State Commun.* **66** 965
[7] Crossley A, Graves P R and Myhra S 1991 *Physica* C **176** 106
[8] Narang S N, Patel N D and Kartha V B 1994 *J. Mol. Struct.* **327** 221
[9] Kuz'menko A B, Tishchenko E A and Orlov V G 1996 *J. Phys.: Condens. Matter* **8** 6199
[10] Chaplot S L 1989 *Phase Transitions* **19** 49
[11] Hardcastle F D and Wachs I E 1992 *J. Solid State Chem.* **97** 319
[12] Boyer L L and Hardy J R 1973 *Phys. Rev.* B **7** 2886
[13] Chaplot S L, Reichardt W, Pinchovius L and Pyka N 1995 *Phys. Rev.* B **52** 7230
[14] Belousov M V 1973 *Fiz. Tverd. Tela* **15** 1206
[15] Kovalev O V 1986 *Irreducible and Induced Representations and Corepresentations of Space Groups* (Moscow: Nauka)
[16] Kuz'menko A B, Tishchenko E A, Orlov V G, Sashin I L and Khlopkin M N 1997 *Int. Conf. on the Physics and Chemistry of Molecular and Oxide Superconductors (Karlsruhe, 1996)* submitted